The fission yeast pleckstrin homology domain protein Spo7 is essential for initiation of forespore membrane assembly and spore morphogenesis

Michiko Nakamura-Kubo[a], Aiko Hirata[b], Chikashi Shimoda[a], and Taro Nakamura[a]
[a]Department of Biology, Graduate School of Science, Osaka City University, Sumiyoshi-ku, Osaka 558-8585, Japan;
[b]Bioimaging Center, Graduate School of Frontier Sciences, University of Tokyo, Kashiwa, Chiba 277-8562, Japan

ABSTRACT **Sporulation in fission yeast represents a unique mode of cell division in which a new cell is formed within the cytoplasm of a mother cell. This event is accompanied by formation of the forespore membrane (FSM), which becomes the plasma membrane of spores. At prophase II, the spindle pole body (SPB) forms an outer plaque, from which formation of the FSM is initiated. Several components of the SPB play an indispensable role in SPB modification, and therefore in sporulation. In this paper, we report the identification of a novel SPB component, Spo7, which has a pleckstrin homology (PH) domain. We found that Spo7 was essential for initiation of FSM assembly, but not for SPB modification. Spo7 directly bound to Meu14, a component of the leading edge of the FSM, and was essential for proper localization of Meu14. The PH domain of Spo7 had affinity for phosphatidylinositol 3-phosphate (PI3P). *spo7* mutants lacking the PH domain showed aberrant spore morphology, similar to that of *meu14* and phosphatidylinositol 3-kinase (*pik3*) mutants. Our study suggests that Spo7 coordinates formation of the leading edge and initiation of FSM assembly, thereby accomplishing accurate formation of the FSM.**

Monitoring Editor
Patrick Brennwald
University of North Carolina

Received: Feb 11, 2011
Revised: Jun 17, 2011
Accepted: Jul 14, 2011

INTRODUCTION

Sporulation in the fission yeast *Schizosaccharomyces pombe* is equivalent to gametogenesis in higher eukaryotes, in that this morphogenetic process accompanies meiotic nuclear division and a cell specialization process culminating in formation of ascospores (Shimoda and Nakamura, 2003; Shimoda, 2004). Ascospores are characterized by their dormancy, a high degree of resistance to environmental stress, and increased genetic diversity. *S. pombe* cells initiate a sporulation program when challenged by nutrient starvation, particularly starvation for nitrogen (Yamamoto *et al.*, 1997). The assembly of a double-unit membrane, called the forespore membrane (FSM), starts during meiosis II. The FSM expands through fusion of membranous vesicles encapsulating a haploid nucleus generated by two rounds of meiotic nuclear division. Spore wall material is then deposited between the inner and outer layers of the FSM (Yoo *et al.*, 1973; Hirata and Tanaka, 1982). The inner layer of the FSM becomes the plasma membrane of newborn spores. The outer layer eventually degrades during sporulation.

One of the most interesting aspects of FSM formation is its initiation because, unlike other biological membranes, the FSM is synthesized de novo within the cytoplasm of the diploid mother cell (Yoo *et al.*, 1973; Hirata and Tanaka, 1982; Tanaka and Hirata, 1982; Nakamura *et al.*, 2001). During meiosis II, FSM formation takes place at the spindle pole body (SPB), which is equivalent to the centrosome of animal cells. The SPB is a proteinaceous structure composed of multiple layers. The *S. pombe* SPB is located in the cytoplasm very close to the nuclear envelope during interphase, but becomes embedded in the nuclear envelope when cells enter

This article was published online ahead of print in MBoC in Press (http://www.molbiolcell.org/cgi/doi/10.1091/mbc.E11-02-0125) on July 20, 2011.

Address correspondence to: Taro Nakamura (taronaka@sci.osaka-cu.ac.jp).

Abbreviations used: CFP, cyan fluorescent protein; DTT, dithiothreitol; EGTA, ethylene glycol tetraacetic acid; FSM, forespore membrane; GEF, guanine nucleotide exchange factor; GFP, green fluorescent protein; GST, glutathione *S*-transferase; HA, hemagglutinin; LEP, leading edge protein; MM, minimal medium; ORF, open reading frame; PH, pleckstrin homology; PI, phosphatidylinositol; PI3P, phosphatidylinositol 3-phosphate; PMSF, phenylmethylsulfonyl fluoride; PS, phosphatidylserine; PSM, prospore membrane; PX, phox homology; SPB, spindle pole body; SSA, sporulation medium; SSL, liquid synthetic medium.

meiosis (Ding *et al.*, 1997). At prophase II, multiple outer plaques are newly formed at the cytoplasmic side of the SPB, as observed by electron microscopy (Hirata and Tanaka, 1982). These morphological alterations of the SPB are referred to as "SPB modification." SPB modification is also detected by anti-Sad1 antibody as a structural alteration of the SPB from a compact dot to a crescent form at a similar stage of meiosis (Hagan and Yanagida, 1995). Although the relationship between the morphological changes observed by electron microscopy and those seen by fluorescence microscopy remains unclear, this SPB modification is presumed to be indispensable for spore formation.

Isolation and characterization of sporulation-related genes (*spo*$^+$) have begun to unveil the molecular mechanism of the initiation of FSM formation (Bresch *et al.*, 1968; Kishida and Shimoda, 1986; Shimoda and Nakamura, 2003; Shimoda, 2004). So far, four meiotic SPB components required for FSM formation have been identified (Takeda and Yamamoto, 1987; Ikemoto *et al.*, 2000; Nakase *et al.*, 2008; Itadani *et al.*, 2010). During vegetative growth, the coiled-coil protein Spo15 is a component of the single-plaque SPB (Ikemoto *et al.*, 2000). The calmodulin orthologue Cam1 is essential for localization of Spo15 to the SPB (Itadani *et al.*, 2010). When meiosis I is initiated, two sporulation-specific proteins, Spo2 and Spo13, are newly produced and recruited to the cytoplasmic side of the SPB dependent on the presence of Spo15. When cells enter meiosis II, meiotic outer plaques, probably composed of Spo2 and Spo13, form at the SPB (SPB modification). Localization of Spo13 to the SPB is dependent on Spo2 (Nakase *et al.*, 2008). The FSM, which is continuously associated with the meiotic outer plaque, expands by fusion with membrane vesicles, and eventually forms a nucleated compartment called the "prespore," a precursor form of the spore. These data show that Spo13 seems to associate closely with the nascent FSM. However, Spo13 is already present at the SPB at meiosis I, considerably earlier than SPB modification. Moreover, Spo13 does not have domains associated with lipid-binding ability (Nakase *et al.*, 2008). Therefore we presume that as yet unknown SPB components that anchor the FSM are involved in meiosis-specific functions.

Morphogenesis of the FSM is also important, as each FSM must accurately encapsulate the dividing nuclei during sporulation. Several proteins involved in FSM morphogenesis have been identified. Pik3/Vps34 is a phosphatidylinositol 3-kinase (PI3K) that catalyzes the production of phosphatidylinositol 3-phosphate (PI3P). Assembly of the FSM still occurs in *pik3*Δ cells, but the cells exhibit a pleiotropic phenotype in FSM formation, such as aberrant starting positions for expansion, disoriented and insufficient expansion, and failure of closure (Takegawa *et al.*, 1995; Onishi *et al.*, 2003b). Although possible targets of PI3P have been identified (Onishi *et al.*, 2003a, 2007; Koga *et al.*, 2004), how this kinase regulates the initiation of FSM formation (i.e., determination of the starting position for expansion) is still unclear. Septins, a conserved family of GTP-binding proteins, are also involved in spore morphogenesis. In metazoan cells, septins are involved in cytokinesis but are also implicated in a variety of other cellular processes, such as vesicular transport, organization of the actin and microtubule cytoskeletons, and oncogenesis (Spiliotis and Nelson, 2006; Hall *et al.*, 2008). There are seven septins in *S. pombe*, three of which (*spn5*$^+$, *spn6*$^+$, and *spn7*$^+$) are induced during sporulation. These septins colocalize interdependently to a ring-shaped structure along each FSM, and their mutation results in disoriented FSM expansion. Therefore these septins appear to form a scaffold that helps to guide oriented expansion of the FSM (Onishi *et al.*, 2010). The leading edge structure of the FSM also plays an important role in encapsulating the dividing nucleus. It is thought that the leading edge is coated with leading edge proteins (LEPs) in both *Saccharomyces cerevisiae* and *S. pombe*. In *S. pombe*, *meu14*$^+$ encodes a LEP. In most *meu14*Δ cells, the FSM forms in inappropriate places, thus failing to encapsulate the nucleus properly, resulting in ascospores that are abnormal in number and shape. Therefore Meu14 is presumed to guide formation of the FSM (Okuzaki *et al.*, 2003).

For proper FSM formation, morphogenesis of the FSM must be strictly regulated in the early stages of FSM formation. Although a number of proteins responsible for either initiation of FSM assembly or FSM shaping have been identified, the question of how these two events are coordinated is not well understood. In this study, we report a novel meiotic SPB component, Spo7, which contains a pleckstrin homology (PH) domain. Our study suggests that Spo7 coordinates formation of the LEP coat and initiation of FSM assembly, thereby accomplishing accurate FSM formation.

RESULTS

spo7$^+$ encodes a protein that has a PH domain

As reported previously, the *spo7-B213* mutant exhibits defects in ascospore formation (Bresch *et al.*, 1968; Figure 1A). To identify the *spo7*$^+$ gene product and its biological function, we isolated the *spo7*$^+$ gene by functional complementation (*Materials and Methods*). A plasmid (pMN(spo7)) was isolated that was able to rescue the sporulation deficiency of *spo7-B213*. Subcloning and partial sequencing revealed that the *spo7*-complementing ability

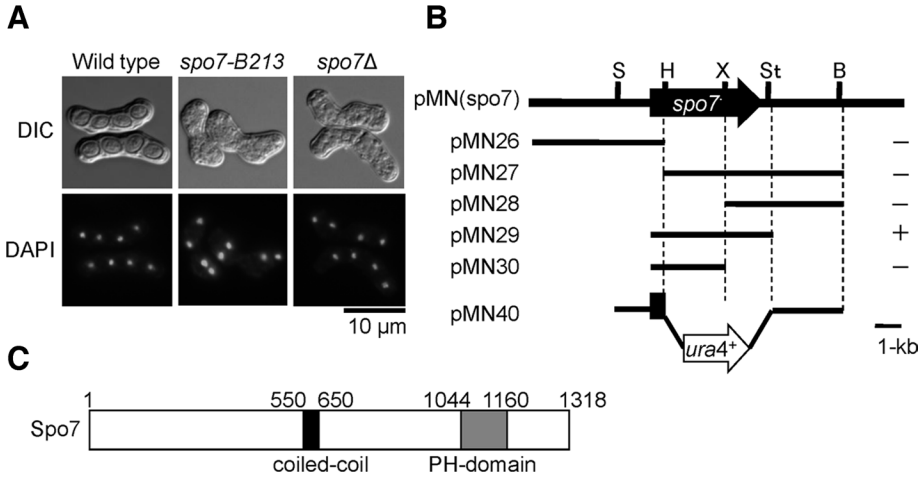

FIGURE 1: Structure of the *spo7*$^+$ gene and predicted protein. (A) Differential interference contrast and DAPI-stained images of *spo7* mutants. MKW5 (wild type), MN4 (*spo7-B213*), and MN8 (*spo7*Δ) strains were incubated at 28°C on SSA for 2 d. Chromosomal DNA was stained with DAPI. (B) Restriction map and subcloning of *spo7*$^+$. Arrow indicates the region and direction of the *spo7*$^+$ ORF, which encodes a protein of 1318 amino acids. All of the subclones were derived from pMN(spo7). Complementation of *spo7-B213* by each subclone: +, complementation; −, no complementation. Restriction enzyme sites: B, *Bgl*II; H, *Hin*dIII; S, *Spe*I; St, *Stu*I. X, *Xho*I. (C) Schematic diagram of Spo7. The coiled-coil region was predicted by using the program COILS with a 21-residue window setting (Lupas *et al.*, 1991). The putative coiled-coil region ($p > 0.8$) is shown as a black box; the PH domain is indicated by a gray box.

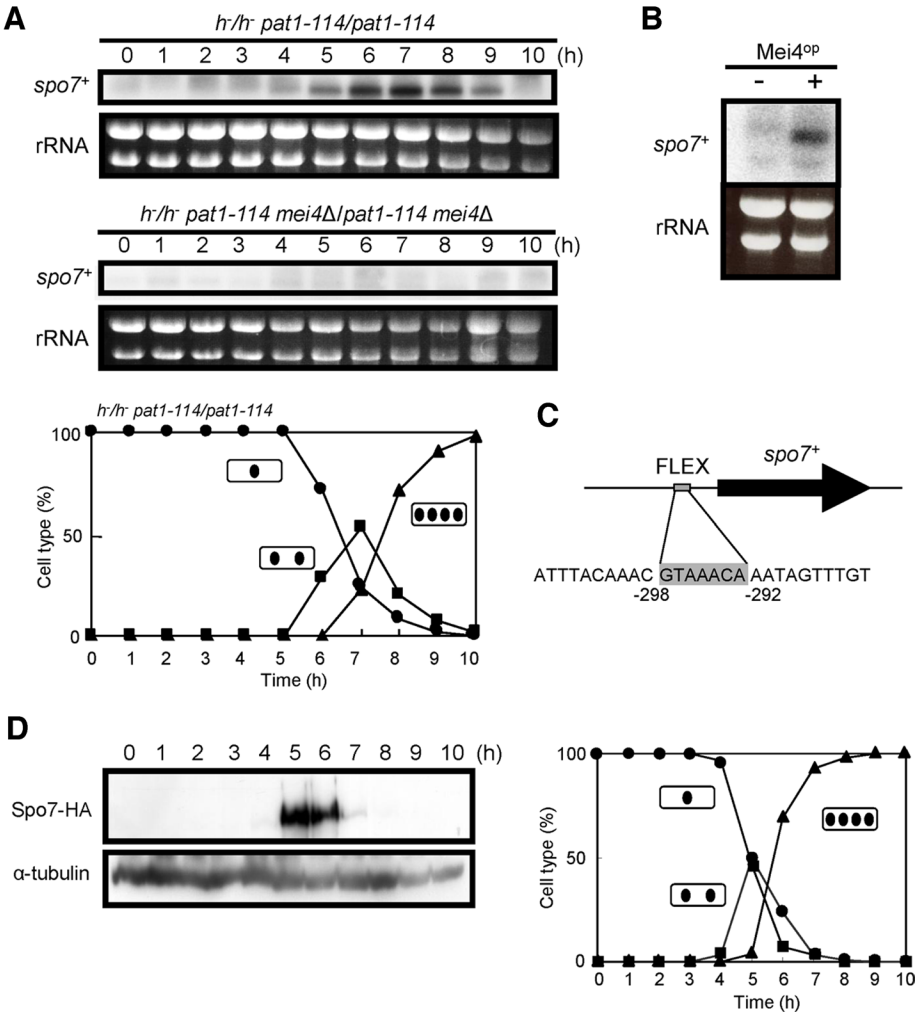

FIGURE 2: Expression of the *spo7*$^+$ gene. (A) Northern analysis of *spo7*$^+$ transcripts in *pat1*-driven meiosis. Synchronous meiosis was initiated in diploid strains homozygous for *pat1-114* (JZ670) and *pat1-114 mei4* (AB4). At hourly intervals, total RNA was prepared (Jensen *et al.*, 1983) and blotted with a radiolabeled *spo7*$^+$ DNA fragment. Meiotic nuclear division of *pat1-114* (JZ670) was monitored by counting the number of nuclei per cell. Circles, mononucleate cells; squares, binucleate cells; triangles, tetranucleate cells. (B) Effect of ectopic expression of *mei4*$^+$ on *spo7*$^+$ transcription. Wild-type cells (TN4) carrying either pREP1 or pREP1(mei4$^+$) were incubated in MM+N at 30°C for 12 h. The approximate quantity of RNA was checked by staining gels with ethidium bromide. (C) Position of the FLEX consensus sequence in the *spo7*$^+$ promoter region. (D) Changes in Spo7 abundance during meiosis. Cells expressing Spo7-HA (MN48) were allowed to proceed through synchronous meiosis. Aliquots were removed at hourly intervals, and the protein extract was subjected to Western blot analysis with the rat anti-HA antibody 3F10 and the anti–α-tubulin antibody TAT-1 as a loading control. Meiotic nuclear division was monitored by counting the number of nuclei per cell. Circles, mononucleate cells; squares, binucleate cells; triangles, tetranucleate cells.

was due to a single open reading frame (ORF; SPAC6G9.04) of 3.9 kb (Figure 1B). This gene is identical to the previously identified gene *mug79*$^+$, which was originally identified as a meiosis-up-regulated gene, but its function has not been well analyzed (Martin-Castellanos *et al.*, 2005). We refer to this gene as *spo7*$^+$ hereafter. The *spo7*$^+$ gene encodes a 150.9-kDa protein consisting of 1318 amino acids. The predicted Spo7 protein has a coiled-coil domain in its central region and a PH domain in its C-terminal region (Figure 1C). The PH domain is found in proteins related to signal transduction, cytoskeleton, membrane trafficking, and lipid modification, and some of these proteins specifically bind to phospholipids (Yu *et al.*, 2004).

To investigate the biological function of *spo7*$^+$, we created a null mutant by conventional gene disruption, using *ura4*$^+$ as a marker (Figure 1B). The *spo7* deletion mutant (*spo7*Δ) was viable, but displayed a sporulation deficiency similar to the original *spo7-B213* mutant (Figure 1A). Because most of the meiosis-defective mutants isolated to date are unable to sporulate (Bresch *et al.*, 1968; Kishida and Shimoda, 1986), we could not rule out the possibility that the *spo7*Δ mutant had a defect in meiosis. Therefore, we analyzed the meiotic nuclear divisions in *spo7*Δ. To synchronize meiosis effectively, we used the *pat1-114* temperature-sensitive strain, which enters meiosis in a highly synchronous manner when it is shifted to its restrictive temperature, 34°C (Iino *et al.*, 1995). The first and second meiotic divisions of the *pat1 spo7*Δ cells were found to proceed with kinetics similar to that observed in *pat1* cells, with the final yield of tetranucleate cells reaching 90% (Supplemental Figure S1). These results suggest that the *spo7*Δ mutant is able to complete meiosis but is defective in ascospore formation.

As mentioned above, *spo7*$^+$/*mug79*$^+$ was originally identified as a gene that is up-regulated in meiosis (Martin-Castellanos *et al.*, 2005). We therefore examined the expression of the *spo7*$^+$ gene in greater detail. Northern blot analysis revealed that *spo7* mRNA was barely detectable in vegetative cells, but accumulated sharply after shifting to nitrogen-free medium (unpublished data. The exact timing of transcriptional induction during sporulation was further explored using the *pat1-114* strain to induce synchronous meiosis. Transcription of *spo7*$^+$ was induced at 5 h after the temperature shift and peaked at 6–7 h, when cells were in meiosis I (Figure 2A). Because the *mei4*$^+$ gene encodes a forkhead transcription factor that regulates many genes required for meiosis and sporulation (Horie *et al.*, 1998; Abe and Shimoda, 2000; Mata *et al.*, 2007), we determined whether Mei4 governs *spo7*$^+$ transcription by examining the induction of *spo7*$^+$ in the *mei4*Δ mutant. As shown in Figure 2A, accumulation of *spo7*$^+$ mRNA was completely abolished in the *mei4*Δ mutant. Furthermore, ectopic overexpression of *mei4*$^+$ induced *spo7*$^+$ mRNA in vegetative cells (Figure 2B). We identified a FLEX-like *cis* element (GTAAACA), which is used by Mei4 to recognize its target (Horie *et al.*, 1998; Abe and Shimoda, 2000), in the 5′ upstream region of the *spo7*$^+$ gene (Figure 2C). Taking these results together, we conclude that transcription of *spo7*$^+$ during meiosis is strictly regulated by Mei4.

The abundance of Spo7 during meiosis was monitored using a chromosomally integrated gene expressing Spo7-hemagglutinin (HA). A single copy of the *spo7-HA* fusion gene completely complemented the sporulation defect of the *spo7*Δ mutant, showing that

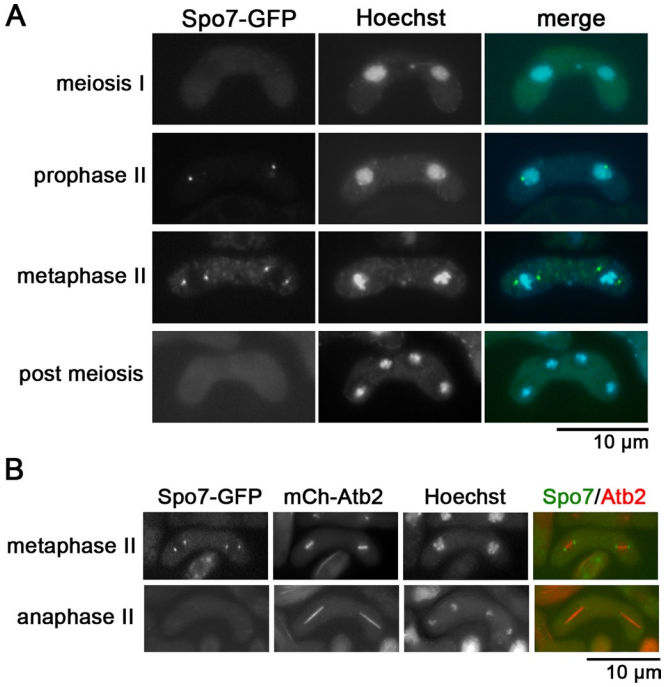

FIGURE 3: Localization of Spo7 during meiosis and sporulation. (A) Localization of Spo7. Homothallic haploid wild-type cells expressing Spo7-GFP (MN10) were sporulated on SSA to induce meiosis. Chromosomal DNA was stained with Hoechst 33342 and analyzed by fluorescence microscopy. Spo7-GFP (green) and Hoechst 33342 (blue) are overlaid in the merged images. (B) Dual observation of Spo7 and microtubules. The homothallic haploid strain TN450 expressing Spo7-GFP and mCherry-Atb2 was sporulated on SSA for 2 d and analyzed by fluorescence microscopy. Spo7-GFP (green) and mCherry-Atb2 (red) are overlaid in the merged images.

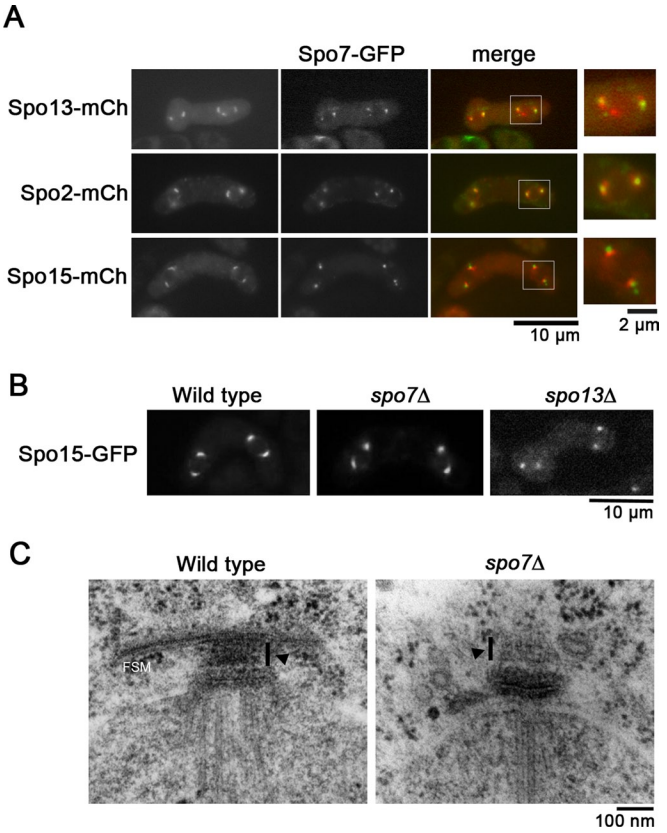

FIGURE 4: Morphological changes in the SPB in *spo7*Δ. (A) Dual observation of Spo7 and other meiotic SPB components. Homothallic haploid strains expressing Spo7-GFP and Spo13-mCherry (TN451), Spo2-mCherry (MN220), or Spo15-mCherry (MN187) were sporulated on SSA for 2 d and analyzed by fluorescence microscopy. Spo7-GFP (green) and Spo13-mCherry, Spo2-mCherry, or Spo15-mCherry (all shown red) are overlaid in the merged images. High-magnification images of the region indicated by the white square are shown on the right. (B) Morphological changes in the *spo7*Δ SPB during meiosis. Wild-type (MN109), *spo7*Δ (MN101), and *spo13*Δ (YN90) were sporulated on SSA. The Spo15-GFP signal in each strain was analyzed by fluorescence microscopy. (C) Fine structures of the SPB in wild-type and *spo7*Δ strains. Wild-type (MKW5) and *spo7*Δ (MN8) cells sporulated on SSA at 28°C for 1 d were observed by electron microscopy. Arrowheads indicate the meiotic outer plaque of the SPB.

Spo7-HA is fully functional. An MN48 strain carrying the *pat1-114* mutation and Spo7-HA was cultured at 34°C to induce synchronous meiosis. Spo7-HA was not detected in vegetative cells (at 0 h), but appeared after the temperature shift (at 5 h) as a 160-kDa band on SDS–PAGE (Figure 2D). This apparent molecular mass was consistent with that deduced from the sequence data. Spo7-HA became more abundant coincident with the appearance of tetranucleate cells (5–6 h). Once meiosis was completed, Spo7-HA was no longer detected. We conclude that Spo7 is transiently produced in meiotic cells.

Spo7 is a novel meiotic component of the SPB

Subcellular localization of Spo7 was observed by fluorescence microscopy. Consistent with the Western blot data, an Spo7–green fluorescent protein (GFP) signal was not observed in vegetative cells or in early meiosis, but appeared in meiosis II as one or two dots in the periphery of nuclei (Figure 3A). These dots were detected at both ends of the spindle microtubules, which were visualized by mCherry-labeled Atb2, at metaphase II (Figure 3B), indicating that Spo7 localizes to the SPB. The Spo7 signal disappeared before spindle breakdown (anaphase II, Figure 3B).

Initiation of FSM formation is regulated by meiotic SPB components, including Spo2, Spo13, and Spo15. To examine the relationship between Spo7 and these other meiotic SPB components, we simultaneously expressed Spo7-GFP and Spo2-mCherry, Spo13-mCherry or Spo15-mCherry in a cell. As shown in Figure 4A, Spo7-GFP was in close contact with each of the three proteins at the SPB. Interestingly, the Spo7-GFP signal was positioned outside the Spo15-mCherry signal at the SPB, but overlapped with Spo2-mCherry and Spo13-mCherry. In addition, the Spo7-GFP signal essentially showed a dot-like pattern but was occasionally accompanied by a faint crescent signal around the dots. However, this pattern was clearly different from those of Spo13-mCherry, Spo2-mCherry, and Spo15-mCherry, which showed a homogeneous crescent signal (Figure 4A). Recruitment of Spo2, Spo13, and Spo15 to the SPB is strictly controlled: localization of Spo13 to the SPB depends on Spo15 and Spo2, whereas that of Spo2 depends only on Spo15 (Nakase *et al.*, 2008). We next examined whether Spo7 localizes to the SPB in mutants of the other meiotic SPB components. As shown in Figure S2A, Spo7 localized to the SPB in each of the *spo2, spo13*, and *spo15* mutant cells. Reciprocally, Spo13, Spo2, and Spo15 each localized to the SPB in *spo7* mutants (Figure S2B). Therefore recruitment of Spo7 to the SPB is independent of other meiotic SPB components. Recently we have shown that the calmodulin orthologue Cam1 regulates initiation of FSM formation by recruiting meiotic

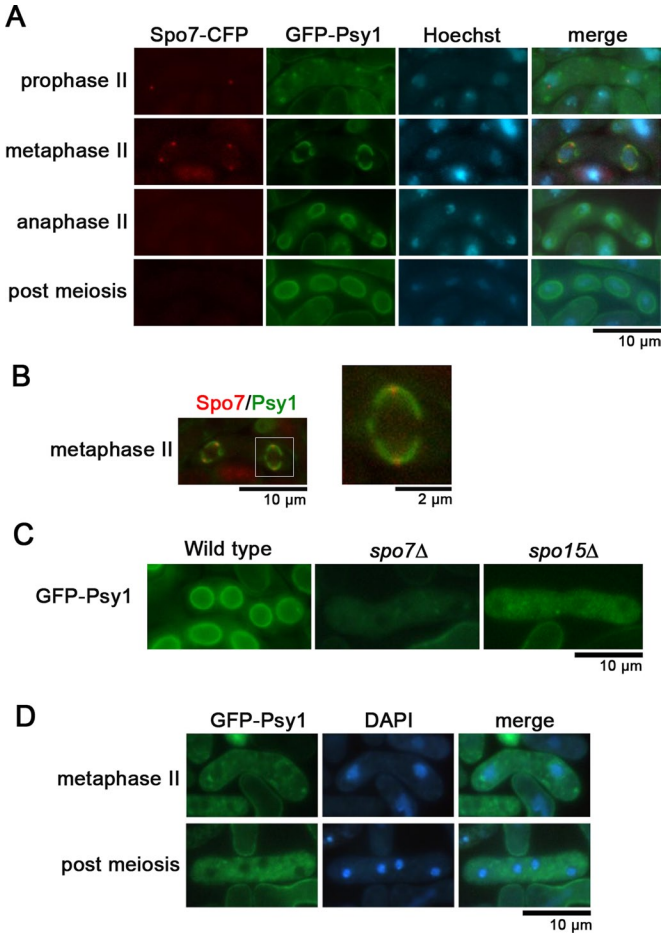

FIGURE 5: FSM formation in *spo7*Δ. (A) Dual observation of Spo7-CFP and the FSM. Wild-type cells (MN56) expressing Spo7-CFP and GFP-Psy1 were sporulated on SSA and were stained with Hoechst 33342. (B) Merged image of Spo7-CFP and the FSM visualized by GFP-Psy1 of (A) (metaphase II). A high-magnification image of the region indicated by the white square is shown on the right. (C) FSM formation in *spo7*Δ. Wild-type (YN68), *spo7*Δ (MN103), and *spo15*Δ (YN67) strains expressing GFP-Psy1 were sporulated on SSA at 28°C for 1 d and were observed by fluorescence microscopy. (D) Initiation of the FSM is defective in *spo7*Δ. *spo7*Δ cells (MN103) expressing GFP-Psy1 were sporulated on SSA at 28°C for 1 d and observed by fluorescence microscopy.

SPB components to the SPB. In *cam1* mutant cells, Spo13, Spo2, and Spo15 all fail to localize to the SPB (Itadani *et al.*, 2010). However, localization of Spo7 at the SPB was not affected by the *cam1* mutation (unpublished data).

We examined the physical interaction of Spo7 with other meiotic SPB components by yeast two-hybrid analysis. The colony formation assay indicated a positive interaction between Spo7 and Spo13. However, no interaction of Spo7 with Spo2 or Spo15 was observed (Figure S2C). The interaction between Spo7 and Spo13 was also detected in *S. pombe* cells (unpublished data). An interaction was also observed between Spo7 and Spo7 (Figure S2C).

We next examined the expression profile of the meiotic SPB components in detail. During meiosis I, an Spo13-GFP signal was observed at the SPB, whereas Spo7-cyan fluorescent protein (CFP) was not detected (Figure S3A), indicating that Spo13 is recruited to the SPB prior to Spo7. Consistently, Western blot analysis showed that both Spo7-HA and Spo13-GFP were expressed exclusively during meiosis II, but Spo13-GFP was expressed slightly earlier than Spo7-HA (Figure S3B).

Spo7 is essential for initiation of FSM formation

Assembly of the FSM initiates in the vicinity of the SPB during meiosis II (Hirata and Tanaka, 1982; Nakamura *et al.*, 2008). Because Spo7 was found to be associated with the SPB prior to spore formation, we presumed that modification of the SPB would be impaired by the *spo7*Δ mutation. Fluorescence microscopic analysis using Spo15-GFP showed that the modified crescent-shaped SPBs were not present in *spo13*Δ cells during the second meiotic division (Figure 4B). Interestingly, unlike *spo13*Δ, most Spo15-GFP signals showed a crescent shape in *spo7*Δ cells (Figure 4B). The fine structures of the meiotic SPB in *spo7*Δ cells were compared with those of the SPB in wild-type strains at the same stage. Our previous study showed that *spo15*Δ cells form no apparent outer plaques (Nakase *et al.*, 2008). Interestingly, as shown in Figure 4C, *spo7*Δ cells seemed to form outer plaques, although the density of these outer plaques seemed to be slightly reduced. Taken together, these data indicate that SPB modification occurs in *spo7*Δ cells.

Assembly of the FSM initiates from the outer plaque of the SPB (Hirata and Tanaka, 1982). To observe Spo7 and the FSM simultaneously, the FSM was visualized by using GFP-tagged Psy1, an FSM-resident protein (Nakamura *et al.*, 2001). The nascent FSM was observed to overlap with Spo7-CFP (Figure 5, A and B), suggesting a close relationship between Spo7 and the FSM. We next examined FSM formation in *spo7*Δ cells. In wild-type cells, the FSM assembled normally as a sac (Figure 5C); by contrast, membrane formation was completely inhibited in *spo7*Δ cells (Figure 5D). This phenotype was similar to that seen in mutants of the other meiotic SPB components such as *spo15* (Figure 5C; Nakase *et al.*, 2008). Furthermore, electron microscopy showed that no FSM was observed near the SPB in *spo7*Δ cells, although membrane vesicles were observed (Figure 4B). Taken together, these data suggest that Spo7 is indispensable for initiating FSM formation and is associated closely with the nascent FSM.

Spo7 is essential for recruitment of Meu14 to the SPB

To determine the in vivo function of the PH domain of Spo7, we constructed a series of deletion mutants, as well as a point mutant of *spo7* (Figure 6A). These mutant *spo7* genes were introduced into the *leu1*locus in *spo7*Δ cells. The *spo7-ΔC1* mutant, lacking the C-terminal 158 amino acids (Figure 6A), could form spores, but the shapes of the spores were markedly abnormal (unpublished data). Similar results were obtained for the *spo7-ΔC2* mutant, in which both the PH domain and the C-terminal region were deleted (Figure 6, B and C). The *spo7-ΔC3* mutation, lacking the C-terminal 451 amino acids (Figure 6A), completely inhibited FSM formation, similar to the *spo7*Δ mutation (Figure 6, B and C). These data indicate that the C-terminal region of Spo7 is not essential for initiation of FSM assembly but is required for proper shaping of the FSM. The *spo7-ΔC2* mutant protein localized to the SPB (Figure 6D), indicating that the defect in the spore morphology of *spo7-ΔC2* is not due to mislocalization of the protein to the SPB. Interestingly, similar to *spo7*Δ, the *spo7-ΔPH* mutant, lacking only the PH domain (Figure 6A), did not form spores. In other words, the *spo7-ΔPH* mutation exhibited a more severe effect than the *spo7-ΔC2* mutation.

To assess the role of the PH domain, we constructed an additional mutant, *spo7*^{L1153P}, in which a conserved leucine residue (1153) in the PH domain was replaced with proline (Figure 6A). *spo7* ^{L1153P} exhibited a phenotype similar to *spo7-ΔPH* (Figure 6B). These data indicate that the PH domain of Spo7 is not required for initiation

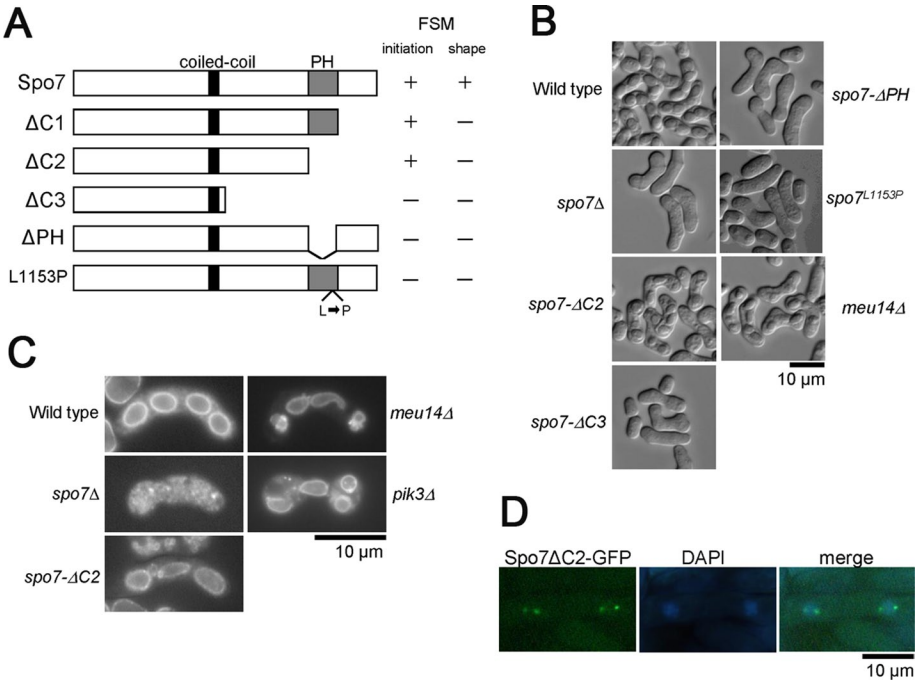

FIGURE 6: Function of the PH domain of Spo7. (A) Schematic illustration of the *spo7* deletion mutants. (B) Sporulation in the *spo7* mutants. Wild-type (YN68), *spo7*Δ (MN103), *spo7-ΔC2* (MN271), *spo7-ΔC3* (MN265), *spo7-ΔPH* (MN263), *spo7*^{L1153P} (MN140), and *meu14*Δ (MN133) cells were sporulated on SSA at 28°C for 2 d. (C) FSM formation in the *spo7* mutants. Wild-type (YN68), *spo7*Δ (MN103), *spo7-ΔC2* (MN271), *spo7-ΔPH* (MN263), *spo7-L1153P* (MN140), and *meu14*Δ (MN133) cells expressing GFP-Psy1 were sporulated on SSA at 28°C for 2 d and observed by fluorescence microscopy. (D) Localization of Spo7ΔC2. Wild-type cells expressing Spo7ΔC2-GFP (MN75) were sporulated on SSA at 28°C for 1 d.

of FSM assembly but is necessary for proper shaping of the FSM. In addition, these data also suggest that the C-terminal region is important for the function of the PH domain. Therefore we subsequently used the *spo7-ΔC2* strain to examine the function of the PH domain.

As mentioned above, two-hybrid analysis showed the dimerization of Spo7. To determine whether dimerization of Spo7 is required for sporulation, we examined the interaction of various *spo7*-deletion mutant proteins with full-length Spo7 using yeast two-hybrid analysis. Whereas Spo7-ΔC2 interacted with Spo7, Spo7-ΔC3 and Spo7-ΔPH did not (Figure S4). Given that *spo7-ΔC2*, but not *spo7-ΔC3* or *spo7-ΔPH*, initiates FSM formation, these data suggest the possibility that Spo7 dimerization is important for FSM initiation.

The phenotype of the *spo7-ΔC2* mutant seemed reminiscent of the prespores with abnormal spore morphology observed in *meu14* mutants. The *meu14*$^{+}$ gene was originally identified as the *meu* gene, the expression of which is up-regulated during meiosis (Watanabe *et al.*, 2001; Okuzaki *et al.*, 2003). Meu14 localizes to the SPB during early meiosis II, and subsequently forms a ring structure at the leading edge of the FSM. The *meu14* null mutant forms spores with an abnormal shape (Figure 6B; Okuzaki *et al.*, 2003). Thus Meu14 plays an important role in spore morphogenesis. Therefore, we examined the relationship between Spo7 and Meu14. First, localization of these proteins was observed. At an early stage of prophase II, Spo7-GFP fluorescence was observed at the SPB, whereas Meu14-mCherry was dispersed in the nucleus (Figure 7A). Subsequently, Meu14-mCherry accumulated at the SPB and was overlapped almost completely by Spo7-GFP, indicating that Spo7 is recruited to the SPB prior to Meu14. At metaphase II, Meu14-mCherry formed ring-like structures, whereas Spo7-GFP persisted at the SPB (Figure 7A).

We next determined the localization of Meu14 in *spo7*Δ cells. Interestingly, in *spo7*Δ cells, Meu14-GFP fluorescence was observed neither at the SPB nor at the leading edge of the FSM, but in the nucleus (Figure 7B). To examine whether the defect in Meu14 localization to the leading edge is a consequence of the defect in FSM formation, we observed the behavior of Meu14-GFP in *spo15*Δ cells, in which FSM formation is completely defective. As shown in Figure 7B, dots and ring-like structures of Meu14-GFP were observed in *spo15* cells, although the size of rings was markedly reduced. Thus, Spo7 is essential for recruitment of Meu14 to the SPB. By contrast, localization of Spo7-GFP was not affected by the *meu14*Δ mutation (Figure 7C).

Next the physical interaction between Spo7 and Meu14 was examined by yeast two-hybrid analysis. The colony formation assay showed that Spo7 positively interacted with Meu14 (Figure 7D). These results led us to analyze potential in vivo interactions in *S. pombe* between Spo7 and Meu14. These polypeptides could not be detected by Western blotting in lysates prepared from sporulating cells. Therefore cell-free extracts were prepared from vegetative cells. Furthermore, because full-length Spo7 was not soluble, a Spo7 cnt polypeptide containing a partial region of Spo7 (aa 363–1043) was coexpressed with Meu14-GFP for these experiments. Spo7cnt-HA was immunoprecipitated with anti-HA antibody, and copurification of Spo7cnt-HA was verified by Western blotting using anti-GFP antibody. As shown in Figure 7E, Meu14-GFP, but not control GFP, was copurified with Spo7cnt-HA, indicating that Spo7 interacts directly with Meu14.

The PH domain of Spo7 has affinity for PI3P

To assess the lipid-binding activity of the Spo7 PH domain, we used a protein–lipid overlay assay (Dower and Mattheakis, 2002). This assay has been used extensively to characterize the lipid-binding specificity of proteins. The PH domain of Spo7 fused with glutathione *S*-transferase (GST) was used to probe a panel of lipids spotted onto nitrocellulose membranes (PIP Strip; Echelon Biosciences, Salt Lake City, UT). As shown in Figure 8, Spo7 specifically bound to PI3P and phosphatidylserine (PS), whereas GST alone showed no detectable binding.

We next examined the role of PI3P in FSM formation. In *S. pombe*, PI3P is produced from phosphatidylinositol (PI) by Pik3, the sole PI3 kinase. PI3P is not detectable in *pik3*Δ cells (Takegawa *et al.*, 1995). The *pik3*Δ mutant shows a pleiotropic phenotype, including a conjugation defect and abnormal vacuole morphology (Takegawa *et al.*, 1995). In addition, *pik3*Δ cells show a defect in sporulation (Onishi *et al.*, 2003a): growth of the FSM in *pik3*Δ cells is incorrectly orientated, failing to engulf the nucleus or forming extremely small spores. Therefore, we next observed the behavior of Meu14 in *pik3*Δ mutants. In wild-type cells, Meu14-GFP was observed as one or two dot(s) at the periphery of each of the two nuclei at early meiosis II (Figure 9A). Although Meu14-GFP dots were also observed in *pik3*Δ

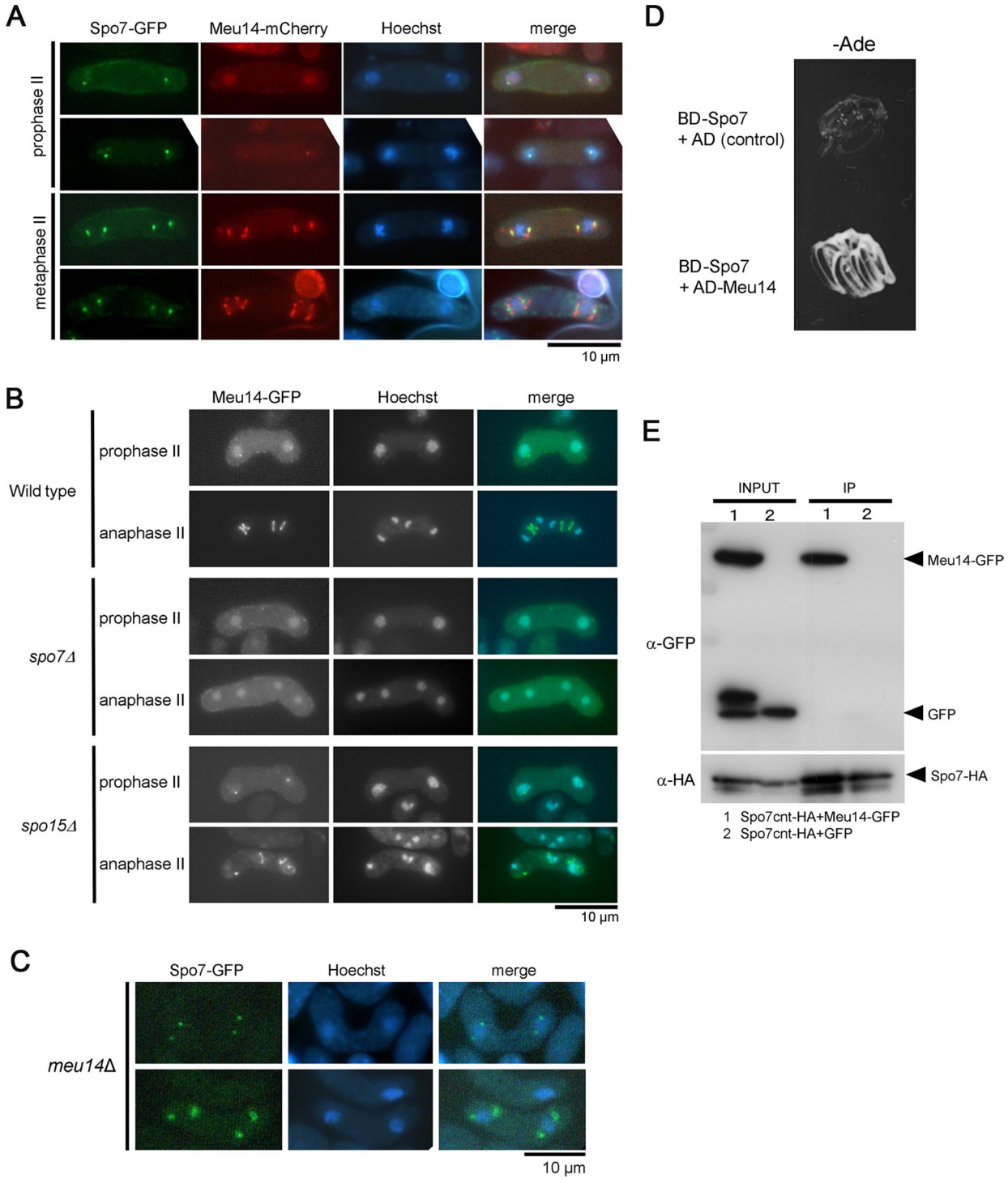

FIGURE 7: Relationship between Spo7 and Meu14. (A) Dual observation of Spo7 and Meu14. Wild-type cells (MN225) expressing integrated Spo7-GFP and Meu14-mCherry were sporulated on SSA at 28°C for 1 d and analyzed by fluorescence microscopy. (B) Localization of Meu14 in *spo7*Δ and *spo15*Δ. Wild-type (YN314), *spo7*Δ (MN156), and *spo15*Δ (MN219) mutants expressing Meu14-GFP were sporulated on SSA at 28°C for 1 d. Meu14-GFP (green) and Hoechst 33342 (blue) are overlaid in the merged images. (C) Localization of Spo7 in *meu14*Δ. *meu14*Δ cells expressing Spo7-GFP (MN77) were sporulated on SSA at 28°C for 1 d and analyzed by fluorescence microscopy. (D) Yeast two-hybrid analysis between Spo7 and Meu14. *spo7*$^+$ was cloned into pGBT9 (Clontech), which contains the DNA-binding domain of the *GAL4* gene (BD). *meu14*$^+$ was cloned into pGAD424 (Clontech), which contains the activation domain of the *GAL4* gene (AD). Plasmids carrying these fusion constructs were introduced into the *S. cerevisiae* tester strain (AH109). The assay was done by monitoring growth of the host cells on adenine-depleted medium. "AD (Control)" indicates pGAD424. (E) Physical interaction between Spo7 and Meu14. GFP or Meu14-GFP was coexpressed with Spo7cnt-HA in wild-type cells (TN29). Whole-cell lysates (input) were subjected to immunoprecipitation with the rat anti-HA antibody 3F10 (IP). Precipitates were analyzed by Western blotting using anti-HA (12CA5) and anti-GFP antibodies.

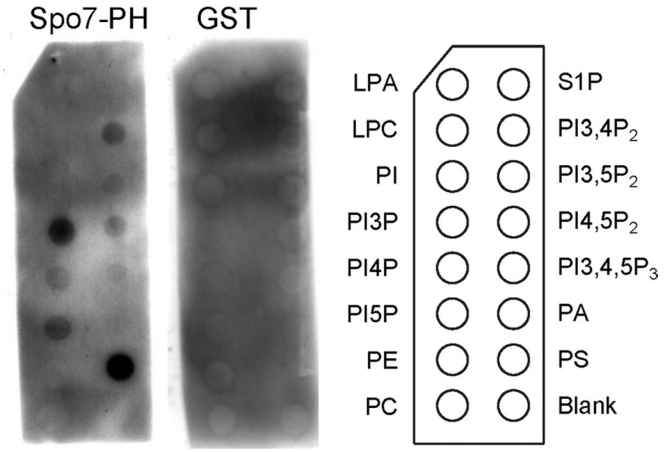

FIGURE 8: Protein–lipid overlay assays using PIP Strips for detecting binding between the indicated lipids and the PH domain of Spo7. Membranes containing the indicated phospholipids (100 pmol per spot) were incubated with the purified GST-Spo7-PH fusion protein or control GST at 200 ng/ml. The membranes were washed, and GST fusion proteins were detected by anti-GST antibody. LPA, lysophosphatidic acid; S1P, sphingosine-1-phosphate; LPC, lysophosphatidylcholine; PI; PA, phosphatidic acid; PE, phosphatidylethanolamine; PS; PC, phosphatidylcholine.

cells, the number of dots in each nucleus was often more than two; in addition, the size of the Meu14-GFP dots in each nucleus differed considerably (Figure 9A). During FSM expansion in wild-type cells, four Meu14-GFP rings localized at the leading edge of the FSM sac and expanded in a synchronous manner (Figure 9B). In *pik3*Δ cells, by contrast, abnormal Meu14 rings caused by loss of synchrony were observed. Furthermore, the Meu14 rings were often fragmented (Figure 9B). Thus these data indicate that PI3P is important for proper assembly of the Meu14 ring. Spo7-GFP localized properly to the SPB in *pik3*Δ cells (Figure 9C), suggesting that the abnormal localization of Meu14 is not due to the mislocalization of Spo7 to the SPB.

We also examined the behavior of Meu14 in the *spo7-ΔC2* mutant lacking the PH domain. Unlike in *spo7*Δ cells, Meu14 rings were observed in *spo7-ΔC2* cells. However, formation of the Meu14 dots and rings was apparently abnormal in *spo7-ΔC2* cells, similar to *pik3*Δ cells (Figure 9, A and B). Taken together, these data suggest that the PH domain of Spo7 is important for proper assembly of Meu14 protein, which is critical to shaping of the FSM.

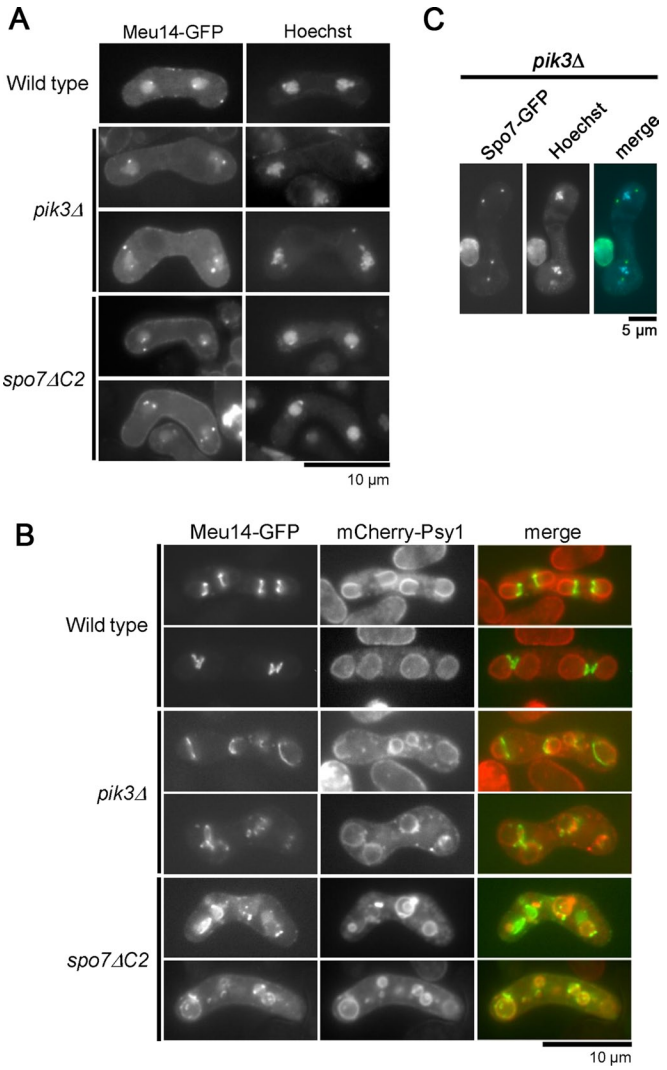

FIGURE 9: Abnormal FSM formation in *spo7ΔC2* and *pik3*Δ. (A) Localization of Meu14 in early meiosis II. Wild-type (TN443), *spo7ΔC2* (TN444), and *pik3*Δ (TN445) cells expressing Meu14-GFP were sporulated on SSA at 28°C for 1 d, stained with Hoechst 33342, and analyzed by fluorescence microscopy. (B) FSM formation in *spo7ΔC2* and *pik3*Δ. Wild-type (TN443), *spo7ΔC2* (TN444), and *pik3*Δ (TN445) cells expressing Meu14-GFP and mCherry-Psy1 were sporulated on SSA at 28°C for 1 d and analyzed by fluorescence microscopy. Meu14-GFP (green) and GFP-Psy1 (red) are overlaid in the merged images. (C) Localization of Spo7-GFP in *pik3*Δ. *pik3*Δ (TN449) cells expressing Spo7-GFP were sporulated on SSA at 28°C for 1 d, stained with Hoechst 33342, and analyzed by fluorescence microscopy. Spo7-GFP (green) and Hoechst 33342 (blue) are overlaid in the merged images.

DISCUSSION

The SPB serves as a platform for FSM assembly in addition to its function as a microtubule-organizing center. The present study raises the possibility that Spo7 is the most membrane-proximal protein among the known meiotic SPB components for the following reasons. First, Spo7 was exclusively produced at meiosis II, a stage when SPB modification and initiation of FSM formation occur, whereas other meiotic SPB components, including Cam1, Spo15, Spo2, and Spo13 are present at the SPB from meiosis I onwards. Second, Spo7 was observed by fluorescence microscopy to localize at the outermost region of the cytoplasmic side of the SPB and to overlap with the FSM. Third, the *spo7*Δ mutation completely inhibited FSM formation, but not SPB modification. In contrast, neither SPB modification nor FSM formation occurs in mutants of other meiotic SPB components (Ikemoto *et al.*, 2000; Nakase *et al.*, 2008; Itadani *et al.*, 2010). At present, however, the mechanism by which Spo7 initiates assembly of the FSM remains unclear. Recently Yang and Neiman (2010) reported that Spo13 acts as a guanine nucleotide exchange factor (GEF) for the small Rab GTPase. Although the in vivo target of Spo13 is unknown, Spo13 binds preferentially to the nucleotide-free form of Ypt2, an orthologue of *S. cerevisiae* Sec4, which regulates vesicle trafficking from the late Golgi to the plasma membrane (Yang and Neiman, 2010). These results demonstrate that stimulation of Rab GTPase activity is essential for initiation of FSM formation. Because Spo7 interacted with Spo13, Spo7 might be involved in the initiation of FSM assembly by regulating the activity of Rab GTPase. Further studies will be required to identify

molecules that physically interact with the Spo7 protein during initiation of FSM formation.

Unexpectedly, the PH domain of Spo7 was not essential for initiation of FSM assembly. The *spo7-ΔC2* mutant, which lacks the C-terminal region including the PH domain, showed a phenotype similar to that of *meu14Δ* and *pik3Δ* mutants with regard to defects in spore morphology. Meu14 first collects at the SPB, and subsequently forms a ring structure at the leading edge of the FSM sac (Okuzaki *et al.*, 2003). Therefore the accumulation of Meu14 at the SPB might be a prerequisite for localization to the leading edge (Okuzaki *et al.*, 2003). Spo7 physically interacted with Meu14 and was essential for localization of Meu14 to the SPB. However, Meu14 rings, albeit small, were formed in *spo15Δ* cells, indicating that assembly of leading edge proteins does not require FSM formation. We suggest that Spo7 has at least two independent roles in sporulation: one is the initiation of FSM formation, and the other is the recruitment of Meu14 to the SPB. Because Spo7 can localize to the SPB in *spo15Δ* cells, we presume that the Meu14 ring can be assembled even in the absence of the FSM. Thus, Spo7 might coordinate the formation of the Meu14 ring and the initiation of FSM assembly, possibly ensuring the precise spatial and temporal control of spore shape.

Our protein–lipid overlay assay showed that the PH domain of Spo7 bound to PI3P. It is known that *pik3Δ* cells exhibit defects in various steps of FSM formation, such as aberrant starting positions for expansion, disoriented FSM expansion, inefficient FSM expansion, and failure of closure of the leading edge (Onishi *et al.*, 2003a). Some of the possible targets of PI3P during sporulation have been identified, including two sorting nexins, Vps5 and Vps17, and the FYVE domain–containing protein Sst4/Vps27. Vps5 and Vps17 have a phox homology (PX) domain, and analysis of homologues of these proteins in *S. cerevisiae* suggests that Vps5 and Vps17 in *S. pombe* act as PI3P-dependent mediators of retrograde trafficking from the endosome to the Golgi apparatus, which in turn acts as an efficient anterograde membrane flux to the FSM (Horazdovsky *et al.*, 1997; Pfeffer, 2001; Onishi *et al.*, 2003a; Koga *et al.*, 2004). In contrast, Sst4 functions at later stages of FSM formation, specifically when the FSM closes (Onishi *et al.*, 2007). However, the target of PI3P that regulates spore morphology at the initial step of FSM formation is still unknown. Interestingly, previous studies by electron microscopy have shown that the tips of the FSM are swollen and fuzzy in *pik3Δ* cells (Onishi *et al.*, 2003a). These abnormal tips are also observed in *meu14Δ* cells (Okuzaki *et al.*, 2003). Indeed, our results indicated that the Meu14 ring is often abnormally assembled in *pik3Δ* cells. Therefore, the most plausible possibility is that PI3P is involved in leading edge ring formation via the PH domain of Spo7. At present, however, we have no evidence that PI3P directly regulates Spo7 in vivo. PH domains have been suggested to bind many proteins, but to date their only clearly demonstrated physiological function is to bind membrane phospholipids (Yu *et al.*, 2004). These facts suggest another possibility: the C-terminal or the PH domain of Spo7 may directly interact with Meu14. However, an Spo7 mutant lacking PH domain still interacted with Meu14 (Figure 7E). We presume that PI3P might influence the interaction between Spo7 and Meu14, thereby facilitating accurate formation of the Meu14 ring and initiation of FSM assembly from the SPB.

The protein–lipid overlay assay also showed that the PH domain interacts with PS, a quantitatively minor phospholipid in eukaryotic cells. *S. pombe* has a sole PS synthase, Pps1. In medium lacking ethanolamine, *pps1Δ* mutants exhibit striking cell morphology, with defects in cytokinesis, actin cytoskeleton cell wall remodeling, and integrity (Matsuo *et al.*, 2007). The phenotype of *pps1Δ* in sporulation has not been investigated. At present, we cannot rule out the possibility that Spo7 is involved in sporulation via binding to PS; however, we presume that PI3P is more important for sporulation, because the phenotype of *spo7-ΔC2* cells was similar to that of *pik3Δ* cells.

It is known that PI3P also plays an important role in autophagy, a major eukaryotic process by which bulk cytoplasmic components are degraded in the vacuole/lysosome. In response to starvation, membrane structures known as autophagosomes nonselectively envelop a fraction of the cytoplasm, including its resident organelles, and target the fraction to the vacuole/lysosome, where the contents are degraded to recycle the components. Like sporulation, formation of the autophagosome is accompanied by de novo assembly of a double-unit membrane (Baba *et al.*, 1994). PI3P is also required for initiation of autophagosomal membrane formation. Thus, regulation of the initiation of membrane assembly by PI3P might be a general mechanism in eukaryotes.

In *S. cerevisiae*, initiation of the prospore membrane (PSM), which corresponds to the FSM, is very similar to that in *S. pombe*: PSM formation begins with a modification of the SPB, and the membrane vesicles gather at the modified SPB and fuse to expand the membrane (Byers, 1981; Neiman, 2005). Four meiotic SPB components, Mpc54p, Mpc70p/Spo21p, Spo74p, and Ady4p, are known to localize at the outer plaque of the SPB and are essential for initiation of PSM assembly (Knop and Strasser, 2000; Bajgier *et al.*, 2001; Nickas *et al.*, 2003). Despite their similar roles in sporulation, however, these proteins share no similarity with *S. pombe* components of the meiotic SPB and do not have domains suggesting lipid-binding ability. A physical interaction between meiotic SPB components and LEPs is also observed in *S. cerevisiae*. Furthermore, deletion of *SSP1*, an LEP, causes defects in spore morphogenesis: PSMs are still formed, but they are grossly abnormal. The membranes occasionally grow in the wrong direction, resulting in a failure to capture nuclei (Moreno-Borchart *et al.*, 2001). These phenotypes are very similar to those of *meu14Δ* cells. Interestingly, however, *S. cerevisiae* LEPs first appear in the cytoplasm and then gather at the SPB, whereas Meu14 appears in the nucleus. In the present study, Spo7 was essential for recruitment of Meu14 to the SPB, and Meu14 persisted in the nucleus in *spo7* mutants, even when meiosis II progressed. Similar to other meiotic SPB components, a protein homologous to Spo7 does not occur in *S. cerevisiae*. Therefore Spo7 might regulate transport of the LEP Meu14 from the nucleus to the SPB, a process specifically seen in *S. pombe*.

On the basis of the results from the present study, together with previous data, we propose a model in which Spo7 regulates FSM formation. During meiosis I, Spo2 and Spo13 are expressed and localized to the SPB. When meiosis II starts, Spo7 localizes to the SPB at the outermost side and regulates proper assembly of the Meu14 ring. PI3P might regulate Spo7 function. Coincidently, Spo7 also regulates initiation of membrane vesicle fusion at the SPB, possibly by interacting with Spo13. The leading edge may control morphogenesis of the FSM, and is thus required for proper sporulation.

In summary, our results indicate that Spo7 provides a link between initiation of FSM formation and spore morphogenesis. Future studies of the function of Spo7 and this model system will help elucidate the more general questions of how membrane formation initiates and how the FSM obtains its shape in vivo.

MATERIALS AND METHODS

Yeast strains, media, and plasmids

The *S. pombe* strains and plasmids used in this study are listed in Tables 1 and 2, respectively. A sporulation-deficient mutant of *S. pombe*, *spo7-B332*, was originally isolated by Bresch *et al.*

Strain (accession no.)[a]	Genotype[b]	Source
	S. pombe	
B213	*h^{90} spo7-B213 ade6-M210*	Bresch *et al.*, 1968
MKW5 (FY7456)	*h^{90}*	Nakamura-Kubo *et al.*, 2003
MN4 (FY21065)	*h^{90} spo7-B213*	This study
MN8 (FY21067)	*h^{90} spo7::ura4^{+} ura4-D18*	This study
MN10 (FY21068)	*h^{90} spo7-GFP<<LEU2 leu1-32*	This study
MN24 (FY21069)	*h^{90} spo2::ura4^{+} spo7-GFP<<LEU2 leu1-32 ura4-D18*	This study
MN26 (FY21070)	*h^{90} spo13::ura4^{+} spo7-GFP<<LEU2 leu1-32 ura4-D18*	This study
MN28 (FY21071)	*h^{90} spo15::ura4^{+} spo7-GFP<<LEU2 leu1-32 ura4-D18*	This study
MN48 (FY21072)	*h^{-}/h^{-} pat1-114/pat1-114 spo7-HA<<LEU2/ spo7-HA<<LEU2 ade6-M210/ade6-M216 leu1-32/leu1-32 ura4-D18/ura4-D18*	This study
MN49 (FY21073)	*h^{-}/h^{-} pat1-114/pat1-114 spo7::ura4^{+}/spo7::ura4^{+} ade6-M210/ade6-M216 leu1-32/ leu1-32 ura4-D18/ura4-D18*	This study
MN56 (FY21074)	*h^{90} spo7-CFP<<ura4^{+} leu1<<GFP-psy1 leu1-32 ura4-D18*	This study
MN69 (FY21077)	*h^{90} spo7-CFP<<ura4^{+} leu1-32 ura4-D18* pAL(spo13-GFP)	This study
MN75 (FY21079)	*h^{90} spo7ΔC2-GFP<<LEU2 leu1-32*	This study
MN77 (FY21351)	*h^{90} meu14::ura4^{+} spo7-GFP<<LEU2 leu1-32 ura4-D18*	This study
MN78 (FY21352)	*h^{-}/h^{-} pat1-114/pat1-114 spo7-HA<<LEU2/spo7-HA<<LEU2 spo13^{+}/spo13-GFP<<<ura4^{+} ade6-M210/ade6-M216 leu1-32/leu1-32 ura4-D18/ura4-D18*	This study
MN99 (FY21080)	*h^{90} spo7::ura4^{+} leu1^{+}<<spo2-GFP leu1-32 ura4-D18*	This study
MN100 (FY21081)	*h^{90} spo7::ura4^{+} leu1^{+}<<spo13-GFP leu1-32 ura4-D18*	This study
MN101 (FY21082)	*h^{90} spo7::ura4^{+} spo15-GFP<<LEU2 leu1-32 ura4-D18*	This study
MN103 (FY21083)	*h^{90} spo7::ura4^{+} leu1^{+}<<GFP-psy1 leu1-32 ura4-D18*	This study
MN109 (FY21084)	*h^{90} spo15-GFP<<LEU2 leu1-32*	This study
MN133 (FY21086)	*h^{90} meu14::ura4^{+} leu1^{+}<<GFP-psy1 leu1-32 ura4-D18*	This study
MN140 (FY21087)	*h^{90} spo7::ura4^{+} leu1^{+}<<spo7-L1153P leu1-32 ura4-D18*	This study
MN156 (FY21088)	*h^{90} spo7::ura4^{+} leu1^{+}<<meu14-GFP ade6-M216 leu1-32 ura4-D18*	This study
MN187 (FY21353)	*h^{90} spo7-GFP<<ura4^{+} spo15-mCherry<<LEU2 ade6-M216 leu1-32 ura4-D18*	This study
MN219 (FY21091)	*h^{90} spo15::ura4^{+} leu1^{+}<< meu14-GFP leu1-32 ura4-D18*	This study
MN220 (FY21354)	*h^{90} spo7-GFP<<LEU2 spo2-mCherry<<ura4^{+} ade6-M216 leu1-32 ura4-D18*	This study
MN221 (FY21092)	*h^{90} pik3::ura4^{+} leu1^{+}<<meu14-GFP leu1-32 ura4-D18*	This study
MN225 (FY21089)	*h^{90} spo7-GFP<<ura4^{+} leu1^{+}<<meu14-mCherry ade6-M216 leu1-32 ura4-D18*	This study
MN263 (FY21095)	*h^{90} spo7::ura4^{+} leu1^{+}<<spo7ΔPH ade6^{+}<<GFP-psy1 ade6-M216 ura4-D18 leu1-32*	This study
MN265 (FY21096)	*h^{90} spo7::ura4^{+} leu1^{+}<<spo7ΔC3 ade6^{+}<<GFP-psy1 ade6-M216 ura4-D18 leu1-32*	This study
MN271 (FY21097)	*h^{90} spo7::ura4^{+} leu1^{+}<<spo7ΔC2 ade6^{+}<<GFP-psy1 ade6-M216 ura4-D18 leu1-32*	This study
JZ670 (FY7051)	*h^{-}/h^{-} pat1-114/pat1-114 ade6-M210/ade6-M216 leu1-32/leu1-32*	Yamamoto
AB4 (FY7476)	*h^{-}/h^{-} pat1-114/pat1-114 mei4::ura4^{+}/mei4::ura4^{+}ade6-M210/ade6-M216 leu1-32/ leu1-32 ura4-D18/ura4-D18*	Abe and Shimoda, 2000
TN4 (FY7251)	*h^{-} leu1-32*	Nakamura *et al.*, 2001
TN29 (FY7816)	*h^{90} leu1-32 ura4-D18*	Ikemoto *et al.*, 2000
TN443 (FY21098)	*h^{90} meu14-GFP his5<<mCherry-psy1::Knr leu1-32*	This study
TN444 (FY21099)	*h^{90} spo7::ura4^{+} ade6^{+}<<meu14-GFP his5^{+}<<mCherry-psy1::Kn^{r} leu1^{+}<<spo7ΔC2 ade6-M216 leu1-32 ura4-D18*	This study

[a] Accession numbers are from the Yeast Genetic Resource Center of Japan supported by the National BioResource Project (YGRC/NBRP; http:/yeast.lab.nig.ac.jp/nig). The *S. pombe* strains constructed in this study have been deposited with the YGRC/NBRP under the accession numbers shown here.
[b] x << y means that gene y is integrated at gene x.

TABLE 1: Strains used in this study.

(Continues)

Strain (accession no.)[a]	Genotype[b]	Source
TN445 (FY21100)	*h^{90} pik3::ura4^{+} leu1^{+}<< meu14-GFP his5^{+}<<mCherry-psy1::Kn^{r} leu1-32 ura4-D18*	This study
TN449 (FY21355)	*h^{90} pik3::ura4^{+} spo7-GFP<<LEU2 leu1-32 ura4-D18*	This study
TN450 (FY21356)	*h^{90} spo7-GFP<<LEU2 ade6^{+}<<mCherry-atb2 ade6-M216 leu1-32 ura4-D18*	This study
TN451 (FY21357)	*h^{90} spo7-GFP<<LEU2 spo13-mCherry<<ura4^{+} ade6-M216 leu1-32 ura4-D18*	This study
YN67 (FY12205)	*h^{90} spo15::ura4^{+} leu1^{+}<<GFP-psy1 leu1-32 ura4-D18*	Nakase *et al.*, 2008
YN68 (FY12710)	*h^{90} leu1^{+}<<GFP-psy1 leu1-32*	Nakase *et al.*, 2008
YN90 (FY12318)	*h^{90} spo13::ura4^{+} spo15-GFP<<LEU2 leu1-32 ura4-D18*	Nakase *et al.*, 2008
YN314 (FY12492)	*h^{90} meu14-GFP leu1-32*	Nakase *et al.*, 2008
	S. cerevisiae	
AH109	Mata, *ura3-52, his3-200, ade2-101, trp1-901, leu2-3112, gal4Δ, met^{-}, gal80Δ, LYS2::GAL1$_{UAS}$-GAL1$_{TATA}$-HIS3, GAL2$_{UAS}$ -GAL2$_{TATA}$ -ADE2, ura3::MEL1$_{UAS}$ -MEL1 $_{TATA}$ -lacZ*	Clontech (Mountain View, CA)

TABLE 1: Strains used in this study. (Continued)

(1968), and was provided by R. Egel (University of Copenhagen, Copenhagen, Denmark). The media used in this study have been previously described (Egel and Egel-Mitani, 1974; Gutz *et al.*, 1974; Moreno *et al.*, 1991. *S. pombe* cells were grown at 30°C and sporulated at 28°C, unless stated otherwise. Synchronous meiosis was induced by a temperature shift using strains carrying the *pat1-114* allele as described (Iino *et al.*, 1995). *S. cerevisiae* strain AH109 (Clontech) was used for two-hybrid analysis.

Cloning of *spo7*$^{+}$

The *spo7-B332* mutant was transformed with the *S. pombe* genomic library, pTN-L1 (Nakamura *et al.*, 2001), containing partial *Sau*3AI fragments constructed in a multi-copy plasmid, pAL-KS (Tanaka *et al.*, 2000). About 10^5 Leu^{+} transformants were incubated on sporulation medium (SSA). The plates were exposed to iodine vapor (Gutz *et al.*, 1974), and those colonies that turned brown were selected as candidates for sporulation-proficient transformants. The plasmid DNA pMN(spo7) was responsible for the recovery of sporulation ability in *spo7* mutants.

Disruption of the *spo7*$^{+}$ gene

The plasmid used for gene disruption was constructed as follows. A 4.0-kb *Hin*dIII–*Stu*I fragment in the *spo7*$^{+}$ ORF was replaced by *ura4*$^{+}$ (1.7 kb; Figure 1). A 6.0-kb *Spe*I–*Bgl*II fragment containing the disrupted *spo7*::*ura4*$^{+}$ gene was transformed into the strain TN29. Disruption was confirmed by genomic Southern hybridization (unpublished data).

Western blotting

MN48 was cultured in liquid sporulation medium (MM−N) at 25°C for 18 h, and the temperature was shifted to 34°C to induce meiosis. At intervals, portions of the culture were collected and crude cell extracts were prepared as described by Masai *et al.* (1995). Polypeptides were resolved by SDS–PAGE on a 10% gel and then transferred onto a polyvinylidene difluoride membrane (Immobilon-P; Millipore, Billerica, MA). Filters were probed with rat anti-HA antibody (3F10, Roche Diagnostics, Indianapolis, IN) at a 1:1000 dilution. Blots were also probed with the anti-α-tubulin antibody TAT-1 (Woods *et al.*, 1989) to ensure that approximately equal amounts of protein were loaded. Immunoreactive bands were revealed by chemiluminescence (NEN Life Sciences, Boston, MA) with horseradish peroxidase–conjugated goat anti–rat (Biosource International, Camarillo, CA) or anti–mouse (Promega, Madison, WI) immunoglobulin G (IgG).

In vivo protein interaction assay

To assay binding between Spo7 and Meu14, we cotransformed the wild-type strain TN29 with plasmids pREP42(spo7cnt-HA) and pMN231 (pREP41(meu14-GFP)). pTN197 (pREP41(GFP)) was used as a control strain instead of pMN231. Transformants were precultured on SD medium. The cells were then transferred to liquid minimal medium (MM) and grown to midlog phase. The cells were harvested, resuspended in extraction buffer (50 mM Tris-HCl, pH 7.5, 10 mM EDTA, 2 mM ethylene glycol tetraacetic acid [EGTA], 200 mM NaCl, 1% Triton X-100, 1 mM phenylmethylsulfonyl fluoride [PMSF]), and then ruptured with glass beads. The lysate was centrifuged at 13,000 × *g* for 20 min to prepare a soluble fraction. The cell-free homogenates were incubated with rat anti-HA (3F10) antibody at 4°C for 1 h, and then mixed with protein G Sepharose (GE Healthcare, Waukesha, WI). The target proteins were detected by Western blot analysis using mouse anti-HA (12CA5, Roche) and mouse anti-GFP (Roche) antibodies.

Fluorescence microscopy

For fluorescence microscopy, cells were suspended in liquid synthetic medium (SSL) without fixation. For DNA staining, cells were washed with water and stained with Hoechst 33342 at 5 μg/ml for 10 min. After centrifugation, the cells were suspended in SSL medium and observed. Photomicrographs were obtained by using a BX51 fluorescence microscope (Olympus, San Jose, CA) equipped with a Roper Cool SNAP charge-coupled device camera (see Figures 1A, 4B, 5, 6D, 7, A and C, S2, A and B, and S3A) or Hamamatsu ORCA-R2 (see Figure 3, 4A, 6C, 7B, and 9). The filter sets U-MWU (Olympus), U-MWIB (Olympus), CFP-2432B (Semrock, Rochester, NY), and U-MWIG2 (Olympus) were used for Hoechst 33342, GFP, CFP, and mCherry, respectively. Image acquisition and processing was carried out by using Aquacosmos (Hamamatsu) and Photoshop (Adobe, San Jose, CA) software.

Protein–lipid overlay assay

pGEX constructs encoding the PH domain of Spo7 or GST vector alone were transformed into *Escherichia coli* BL21, and a 200-ml culture was grown at 30°C in Luria broth containing 100 μg/ml ampicillin until the absorbance at 600 nm was 0.4–0.5. Isopropyl-β-D-thiogalactoside (100 μM) was added, and the cells were cultured for an additional 4 h at 30°C. The cells were collected and washed once with phosphate-buffered saline at pH 7.4. The cells were then resuspended in 25 ml of ice-cold Buffer A (10 mM

Plasmid	Characteristics	Source
	S. pombe	
pAL-KS	*ars1, LEU2*-based multicopy shuttle vector	Tanaka *et al.*, 2000
pAL(spo13-GFP)	pAL-KS, *spo13-GFP*	Nakase *et al.*, 2008
pIL	*LEU2*-based integration vector	Ikemoto *et al.*, 2000
pIL(spo7-HA)	pIL, *spo7-HA*	This study
pIL(spo7-GFP)	pIL, *spo7-GFP*	This study
pIL(spo7ΔC2-GFP)	pIL, *spo7ΔC2-GFP*	This study
pIL(spo7-CFP)	pIL, *spo7-CFP*	This study
pIL(spo15-GFP)	pIL, spo15-GFP	Nakase *et al.*, 2008
pREP1	ars, *LEU2*-based expression vector carrying *nmt1*$^+$ promoter	Maundrell, 1993
pREP1(mei4)	pKEP1, *mei4*$^+$- coding region	Abe and Shimoda, 2000
pTN197	ars, *LEU2*-based expression vector carrying *nmt41*$^+$ promoter, *GFP*	Nakamura *et al.*, 2001
pMN231	pTN197, *meu14*$^+$	This study
pREP42	ars, *ura4*$^+$-based expression vector carrying *nmt41*$^+$ promoter	Maundrell, 1993
pREP42(spo7cnt-HA)	pREP42, *spo7cnt, HA*	This study
pBR(leu1)	*leu1*$^+$ in pBR322	Nakamura-Kubo *et al.*, 2003
pBR(leu1)(spo7)	pBR(leu1), *spo7*$^+$	This study
pBR(leu1)(spo7ΔC1)	pBR(leu1), *spo7ΔC1*	This study
pBR(leu1)(spo7ΔC2)	pBR(leu1), *spo7ΔC2*	This study
pBR(leu1)(spo7ΔC3)	pBR(leu1), *spo7ΔC3*	This study
pBR(leu1)(spo7ΔPH)	pBR(leu1), *spo7ΔPH*	This study
pBR(leu1)(spo7L1153P)	pBR(leu1), *spo7L1153P*	This study
pBR(leu1)(GFP-psy1)	pBR(leu1), *GFP-psy1*	Nakamura-Kubo *et al.*, 2003
pBR(leu1)(mCherry-psy1)	pBR(leu1), *mCherry-psy1*	This study
pBR(leu1)(spo2-GFP)	pBR(leu1), *spo2-GFP*	Nakase *et al.*, 2008
pBR(leu1)(spo13-GFP)	pBR(leu1), *spo13-GFP*	Nakase *et al.*, 2008
pBR(leu1)(mCherry-psy1)	pBR(leu1), *mCherry-psy1*	This study
pBR(leu1)(meu14-GFP)	pBR(leu1), *meu14-GFP*	Ito
pBR(leu1)(meu14-mCherry)	pBR(leu1), *meu14-mCherry*	This study
pIA	*ade6*$^+$ in pBluescript II KS(−)	Tamai
pIA(mCherry-atb2)	pIA, *nmt1* promoter, *mCherry-atb2*	This study
pIH	*his5*$^+$ in pBluescript II KS(−)	This study
pIH(mCherry-psy1)Kn^r	pIH, *mCherry-psy1*, *Kn*^{r}	This study
pIU(spo13-GFP)	*ura4*$^+$ in pBluescript II KS(−), *spo13-GFP*	This study
pIU(spo13-mCherry)	*ura4*$^+$ in pBluescript II KS(−), *spo13-mCherry*	This study
pIU(spo2- mCherry)	pBR(leu1), *spo7*$^+$	This study
	S. cerevisiae	
pGAD424	2 μ origin, *LEU2*-based vector carrying an activation domain of Gal4 and *ADH1* promoter	Clontech (Mountain View, CA)
pGAD424(meu14)	pGAD424, *meu14*$^+$	This study
pGAD424(spo7)	pGAD424, *spo7*$^+$	This study
ppGAD424(spo2)	pGAD424, *spo2*$^+$	This study
pGAD424(spo13)	pGAD424, *spo13*$^+$	This study
pGAD424(spo15)	pGAD424, *spo15*$^+$	This study
pGBT9	2 μ origin, *TRP1*-based vector carrying a DNA-binding domain of Gal4 and *ADH1* promoter	Clontech (Mountain View, CA)
pGBT9(spo7)	pGBT9, *spo7*$^+$	This study
pGBT9(spo7ΔC2)	pGBT9, *spo7ΔC2*	This study
pGBT9(spo7ΔC3)	pGBT9, *spo7ΔC3*	This study
pGBT9(spo7ΔPH)	pGBT9, *spo7ΔPH*	This study

TABLE 2: Plasmids.

Tris-HCl, pH 7.4, containing 1 M NaCl, 1% Triton X-100, 1 mM dithiothreitol [DTT], 0.5 mM PMSF) and ruptured by sonication. The lysates were centrifuged at 20,000 × *g* for 30 min at 4°C. The supernatant was then filtered through a 0.45 μm filter and incubated for 40 min on a rotating platform with 200 μl of glutathione–Sepharose pre-equilibrated in Buffer A (containing 0.5 M NaCl, 20% glycerol). The suspension was centrifuged for 1 min a 3000 × *g*, and the beads were washed three times with 15 ml of Buffer A containing 0.5 M NaCl, 20% glycerol and then a further six times with 15 ml of Buffer B (20 mM Tris-HCl, pH 7.5, containing 20% glycerol, 100 mM KCl, 0.1% Triton X-100, 1 mM DTT, 0.5 mM PMSF). The protein was eluted from the resin at 4°C by incubation with 0.5 ml of Buffer B containing 20 mM glutathione. The eluate was divided into aliquots and stored at −80°C.

The protein–lipid overlay assay was performed using the GST fusion proteins (GST and GST-Spo7-PH) mentioned above. The membrane was blocked in 3% fatty acid-free bovine serum albumin in TBST (50 mM Tris-HCl, pH 7.5, containing 150 mM NaCl, and 0.1% Tween 20) for 1 h and was then incubated overnight at 4°C with gentle stirring in the same solution containing either 200 ng/ml of GST fusion protein. The membranes were washed six times over 30 min in TBST, and then incubated for 1 h with horseradish peroxidase–conjugated goat with anti–mouse IgG (Sigma). Finally, the membranes were washed 12 times over 1 h in TBST, and GST fusion protein that was bound to the membrane by virtue of its interaction with phospholipid was detected by enhanced chemiluminescence.

Electron Microscopy

Samples for electron microscopy were prepared as described (Ye *et al.*, 2007), and sections were viewed on an electron microscope (H-7600, Hitachi, Tokyo, Japan) at 100 kV.

ACKNOWLEDGMENTS

We thank Masayuki Yamamoto (University of Tokyo, Tokyo, Japan), Kayoko Tanaka (University of Leicester, Leicester, UK), Hiroshi Nojima (Osaka University, Suita, Japan), Kaoru Takegawa (Kyushu University, Fukuoka, Japan), Richard Egel (University of Copenhagen, Copenhagen, Denmark), and Roger Tsien (University of California, San Diego, CA) for strains and plasmids and Keith Gull (University of Oxford, Oxford, UK) for antibody. This study was supported in part by a Grant-in-Aid for Scientific Research (C) and a Grant-in-Aid for Scientific Research on Priority Area "Cell Proliferation Control" from the Ministry of Education, Culture, Sports, Science and Technology of Japan, and the Asahi Glass Foundation (to T.N.). M.N.-K. is a recipient of the Research Fellowship for Young Scientists from the Japan Society for the Promotion of Science.

REFERENCES

Abe H, Shimoda C (2000). Autoregulated expression of *Schizosaccharomyces pombe* meiosis-specific transcription factor Mei4 and a genome-wide search for its target genes. Genetics 154, 1497–1508.

Baba M, Takeshige K, Baba N, Ohsumi Y (1994). Ultrastructural analysis of the autophagic process in yeast: detection of autophagosomes and their characterization. J Cell Biol 124, 903–913.

Bajgier BK, Malzone M, Nickas M, Neiman AM (2001). *SPO21* is required for meiosis-specific modification of the spindle pole body in yeast. Mol Biol Cell 12, 1611–1621.

Bresch C, Muller G, Egel R (1968). Genes involved in meiosis and sporulation of a yeast. Mol Gen Genet 102, 301–306.

Byers B (1981). Cytology of the yeast life cycle. In: The Molecular Biology of the Yeast *Saccharomyces*: Life Cycle and Inheritance, ed. JN Strathern, EW Jones, and JR Broach, New York: Cold Spring Harbor Laboratory, 59–96.

Ding R, West RR, Morphew DM, Oakley BR, McIntosh JR (1997). The spindle pole body of *Schizosaccharomyces pombe* enters and leaves the nuclear envelope as the cell cycle proceeds. Mol Biol Cell 8, 1461–1479.

Dower WJ, Mattheakis LC (2002). In vitro selection as a powerful tool for the applied evolution of proteins and peptides. Curr Opin Chem Biol 6, 390–398.

Egel R, Egel-Mitani M (1974). Premeiotic DNA synthesis in fission yeast. Exp Cell Res 88, 127–134.

Gutz H, Heslot H, Leupold U, Loprieno N (1974). *Schizosaccharomyces pombe*. In: Handbook of Genetics 1, ed. RC King, New York: Plenum, 395–446.

Hagan I, Yanagida M (1995). The product of the spindle formation gene *sad1*$^+$ associates with the fission yeast spindle pole body and is essential for viability. J Cell Biol 129, 1033–1047.

Hall PA, Russell SEH, Pringle JR (2008). The Septins, London: Wiley-Blackwell.

Hirata A, Tanaka K (1982). Nuclear behavior during conjugation and meiosis in the fission yeast *Schizosaccharomyces pombe*. J Gen Appl Microbiol 28, 263–274.

Horazdovsky BF, Davies BA, Seaman MN, McLaughlin SA, Yoon S, Emr SD (1997). A sorting nexin-1 homologue, Vps5p, forms a complex with Vps17p and is required for recycling the vacuolar protein-sorting receptor. Mol Biol Cell 8, 1529–1541.

Horie S, Watanabe Y, Tanaka K, Nishiwaki S, Fujioka H, Abe H, Yamamoto M, Shimoda C (1998). The *Schizosaccharomyces pombe mei4*$^+$ gene encodes a meiosis-specific transcription factor containing a forkhead DNA-binding domain. Mol Cell Biol 18, 2118–2129.

Iino Y, Hiramine Y, Yamamoto M (1995). The role of *cdc2* and other genes in meiosis in *Schizosaccharomyces pombe*. Genetics 140, 1235–1245.

Ikemoto S, Nakamura T, Kubo M, Shimoda C (2000). *S. pombe* sporulation-specific coiled-coil protein Spo15p is localized to the spindle pole body and essential for its modification. J Cell Sci 113, 545–554.

Itadani A, Nakamura T, Hirata A, Shimoda C (2010). *Schizosaccharomyces pombe* calmodulin, Cam1, plays a crucial role in sporulation by recruiting and stabilizing the spindle pole body components responsible for assembly of the forespore membrane. Eukaryot Cell 9, 1925–1935.

Jensen R, Sprague GF Jr, Herskowitz I (1983). Regulation of yeast mating-type interconversion: feedback control of HO gene expression by the mating-type locus. Proc Natl Acad Sci USA 80, 3035–3039.

Kishida M, Shimoda C (1986). Genetic mapping of eleven *spo* genes essential for ascospore formation in the fission yeast *Schizosaccharomyces pombe*. Curr Genet 10, 443–447.

Knop M, Strasser K (2000). Role of the spindle pole body of yeast in mediating assembly of the prospore membrane during meiosis. EMBO J 19, 3657–3667.

Koga T, Onishi M, Nakamura Y, Hirata A, Nakamura T, Shimoda C, Iwaki T, Takegawa K, Fukui Y (2004). Sorting nexin homologues are targets of phosphatidylinositol 3-phosphate in sporulation of *Schizosaccharomyces pombe*. Genes Cells 9, 561–574.

Lupas A, Van Dyke M, Stock J (1991). Predicting coiled coils from protein sequences. Science 252, 1162–1164.

Martin-Castellanos C *et al.* (2005). A large-scale screen in *S. pombe* identifies seven novel genes required for critical meiotic events. Curr Biol 15, 2056–2062.

Masai H, Miyake T, Arai K (1995). *hsk1*$^+$, a *Schizosaccharomyces pombe* gene related to *Saccharomyces cerevisiae CDC7*, is required for chromosomal replication. EMBO J 14, 3094–3104.

Mata J, Wilbrey A, Bahler J (2007). Transcriptional regulatory network for sexual differentiation in fission yeast. Genome Biol 8, R217.

Matsuo Y, Fisher E, Patton-Vogt J, Marcus S (2007). Functional characterization of the fission yeast phosphatidylserine synthase gene, *pps1*, reveals novel cellular functions for phosphatidylserine. Eukaryot Cell 6, 2092–2101.

Maundrell K (1993). Thiamine-repressible expression vectors pREP and pRIP for fission yeast. Gene 123, 127–130.

Moreno S, Klar A, Nurse P (1991). Molecular genetic analysis of fission yeast *Schizosaccharomyces pombe*. Methods Enzymol 194, 793–823.

Moreno-Borchart AC, Strasser K, Finkbeiner MG, Shevchenko A, Knop M (2001). Prospore membrane formation linked to the leading edge protein (LEP) coat assembly. EMBO J 20, 6946–6957.

Nakamura T, Asakawa H, Nakase Y, Kashiwazaki J, Hiraoka Y, Shimoda C (2008). Live observation of forespore membrane formation in fission yeast. Mol Biol Cell 19, 3544–3553.

Nakamura T, Nakamura-Kubo M, Hirata A, Shimoda C (2001). The *Schizosaccharomyces pombe spo3*$^+$ gene is required for assembly of the forespore membrane and genetically interacts with *psy1*$^+$ encoding syntaxin-like protein. Mol Biol Cell 12, 3955–3972.

Nakamura-Kubo M, Nakamura T, Hirata A, Shimoda C (2003). The fission yeast *spo14*$^{+}$ gene encoding a functional homologue of budding yeast Sec12 is required for the development of forespore membranes. Mol Biol Cell 14, 1109–1124.

Nakase Y, Nakamura-Kubo M, Ye Y, Hirata A, Shimoda C, Nakamura T (2008). Meiotic spindle pole bodies acquire the ability to assemble the spore plasma membrane by sequential recruitment of sporulation-specific components in fission yeast. Mol Biol Cell 19, 2476–2487.

Neiman AM (2005). Ascospore formation in the yeast *Saccharomyces cerevisiae*. Microbiol Mol Biol Rev 69, 565–584.

Nickas ME, Schwartz C, Neiman AM (2003). Ady4p and Spo74p are components of the meiotic spindle pole body that promote growth of the prospore membrane in *Saccharomyces cerevisiae*. Eukaryot Cell 2, 431–445.

Okuzaki D, Satake W, Hirata A, Nojima H (2003). Fission yeast *meu14*$^{+}$ is required for proper nuclear division and accurate forespore membrane formation during meiosis II. J Cell Sci 116, 2721–2735.

Onishi M, Iida M, Koga T, Yamada S, Hirata A, Iwaki T, Takegawa K, Fukui Y, Tachikawa H (2007). *Schizosaccharomyces pombe* Sst4p, a conserved Vps27/Hrs homolog, functions downstream of phosphatidylinositol 3-kinase Pik3p to mediate proper spore formation. Eukaryot Cell 6, 2343–2353.

Onishi M *et al.* (2010). Role of septins in the orientation of forespore membrane extension during sporulation in fission yeast. Mol Cell Biol 30, 2057–2074.

Onishi M, Koga T, Morita R, Nakamura Y, Nakamura T, Shimoda C, Takegawa K, Hirata A, Fukui Y (2003a). Role of phosphatidylinositol 3-phosphate in formation of forespore membrane in *Schizosaccharomyces pombe*. Yeast 20, 193–206.

Onishi M, Nakamura Y, Koga T, Hirata A, Fukui Y (2003b). Importance of phosphatidylinositol 3-phosphate in sporulation of *Schizosaccharomyces pombe*. Biosci Biotechnol Biochem 67, 1191–1193.

Pfeffer SR (2001). Membrane transport: retromer to the rescue. Curr Biol 11, R109–R111.

Shimoda C (2004). Forespore membrane assembly in yeast: coordinating SPBs and membrane trafficking. J Cell Sci 117, 389–396.

Shimoda C, Nakamura T (2003). Control of late meiosis and ascospore formation. In: The Molecular Biology of *Schizosaccharomyces pombe,* ed. R Egel, New York: Springer, 311–327.

Spiliotis ET, Nelson WJ (2006). Here come the septins: novel polymers that coordinate intracellular functions and organization. J Cell Sci 119, 4–10.

Takeda T, Yamamoto M (1987). Analysis and in vivo disruption of the gene coding for calmodulin in *Schizosaccharomyces pombe*. Proc Natl Acad Sci USA 84, 3580–3584.

Takegawa K, DeWald DB, Emr SD (1995). *Schizosaccharomyces pombe* Vps34p, a phosphatidylinositol-specific PI 3-kinase essential for normal cell growth and vacuole morphology. J Cell Sci 108, 3745–3756.

Tanaka K, Hirata A (1982). Ascospore development in the fission yeasts *Schizosaccharomyces pombe* and *S. japonicus*. J Cell Sci 56, 263–279.

Tanaka K, Yonekawa T, Kawasaki Y, Kai M, Furuya K, Iwasaki M, Murakami H, Yanagida M, Okayama H (2000). Fission yeast Eso1p is required for establishing sister chromatid cohesion during S phase. Mol Cell Biol 20, 3459–3469.

Watanabe T, Miyashita K, Saito TT, Yoneki T, Kakihara Y, Nabeshima K, Kishi YA, Shimoda C, Nojima H (2001). Comprehensive isolation of meiosis-specific genes identifies novel proteins and unusual non-coding transcripts in *Schizosaccharomyces pombe*. Nucleic Acids Res 29, 2327–2337.

Woods A, Sherwin T, Sasse R, MacRae TH, Baines AJ, Gull K (1989). Definition of individual components within the cytoskeleton of *Trypanosoma brucei* by a library of monoclonal antibodies. J Cell Sci 93, 491–500.

Yamamoto M, Imai Y, Watanabe Y (1997). Mating and sporulation in *Schizosaccharomyces pombe*. In: Molecular and Cellular Biology of the Yeast *Saccharomyces,* ed. JR Pringle, JB Broach, and EW Jones, New York: Cold Spring Harbor Laboratory, 1037–1106.

Yang HJ, Neiman AM (2010). A guanine nucleotide exchange factor is a component of the meiotic spindle pole body in *Schizosaccharomyces pombe*. Mol Biol Cell 21, 1272–1281.

Ye Y, Fujii M, Hirata A, Kawamukai M, Shimoda C, Nakamura T (2007). Geranylgeranyl diphosphate synthase in fission yeast is a heteromer of farnesyl diphosphate synthase (FPS), Fps1, and an FPS-like protein, Spo9, essential for sporulation. Mol Biol Cell 18, 3568–3581.

Yoo BY, Calleja GB, Johnson BF (1973). Ultrastructural changes of the fission yeast (*Schizosaccharomyces pombe*) during ascospore formation. Arch Mikrobiol 91, 1–10.

Yu JW, Mendrola JM, Audhya A, Singh S, Keleti D, DeWald DB, Murray D, Emr SD, Lemmon MA (2004). Genome-wide analysis of membrane targeting by *S. cerevisiae* pleckstrin homology domains. Mol Cell 13, 677–688.